Facile Fabrication of Uniform Core–Shell Structured Carbon Nanotube–Polyaniline Nanocomposites

ARTICLE *in* THE JOURNAL OF PHYSICAL CHEMISTRY C · APRIL 2009

Impact Factor: 4.77 · DOI: 10.1021/jp808582f

7 AUTHORS, INCLUDING:

li li
Texas Tech University
12 PUBLICATIONS **330** CITATIONS
SEE PROFILE

Zongyi Qin
Donghua University
83 PUBLICATIONS **722** CITATIONS
SEE PROFILE

Facile Fabrication of Uniform Core−Shell Structured Carbon Nanotube−Polyaniline Nanocomposites

Li Li,[†,‡] Zong-Yi Qin,*[,†,‡] Xia Liang,[†] Qing-Qing Fan,[†] Ya-Qing Lu,[‡] Wen-Hua Wu,[‡] and Mei-Fang Zhu*[,†]

State Key Laboratory for Modification of Chemical Fibers and Polymer Materials, and College of Material Science and Engineering, Donghua University, Shanghai 200051, People's Republic of China

Received: September 27, 2008; Revised Manuscript Received: February 05, 2009

The effective site-selective interaction between the π-bonds in the aromatic rings of the polyaniline and the graphitic structure of multiwall carbon nanotubes would strongly facilitate the charge-transfer reaction between the two components. We adopted multiwall carbon nanotubes (MWNTs) with minimal defects as templates and facilely fabricated carbon nanotube−polyaniline nanocomposites with uniform core−shell structures by ultrasonic assisted in situ polymerization. By varying the ratio of aniline monomers and carbon nanotubes, the thickness of polyaniline layers can be effectively controlled. The results indicated that the presence of carbon nanotubes with minimized defects induced the formation of a more planar conformation of polyaniline even when a high weight percent of aniline was loaded. As a result, macroscopically, great improvements in the electrical and electrochemical properties of the resulting nanocomposites were observed.

1. Introduction

The nanocomposites of carbon nanotubes and conductive polymers have attracted more and more attention due to the synergistic effects between these components during the past two decades.[1−5] For polymers, based on the template effects of the carbon nanotubes, very high specific surface area of polymer layers can be obtained, especially the expected high oriented polymer molecules along carbon nanotubes. Meanwhile, for carbon nanotubes, the addition of polymers would be helpful for improving the thermoforming process of the composites. By integrating the excellent properties of these two materials, it would occupy a large advantage for their potential application in chemistry and physics, particularly for the development of new nanotechnologies and devices.

The reason that the conductive polymers were the best candidate to fabricate the hybrid materials was the conjugated groups of polymers, which would interact strongly with the planar graphite of carbon nanotubes. Many researchers have reported about the compact combination of carbon nanotubes and conductive polymers including polypyrrole, polythiophene, and polyaniline.[6−8] Among theses conductive polymers, polyaniline (PANI) was an outstanding candidate for application as electrodes materials in battery and supercapacitor, electrochemical sensor, and hydrogen storage materials, due to its environmental stability and controllable conductivity over a wide range by protonation and charge-transfer doping.[9−11] Moreover, the low price of aniline monomers and good processability of polyaniline should provide more reliable promises for applications.

Considerable achievements have been made in enhancing the electrical and mechanical properties of polymer−carbon nanotubes nanocomposites. Various methods for enhancing the interaction between polymer and carbon nanotubes that mainly included covalent and noncovalent combination were studied by researchers. To get a covalent combination, polymer was usually grafted to the defect sites on the side-wall of the carbon nanotube.[12] For obtaining more reaction sites, carbon nanotubes were usually treated in a strong inorganic acid-like mixture of H_2SO_4 and HNO_3 to introduce active groups such as carboxyl.[13] It is desirable to disperse carbon nanotubes homogeneously throughout the polymer matrix while avoiding damage to their integrity for utilizing effectively the carbon nanotubes as filler materials either for conductive or for mechanical properties. Unfortunately, these treatment processes in mixed acids were very severe, the carbon nanotubes usually were cut into pieces, and a large number of unwanted defects appeared on the side-wall surface of carbon nanotubes. These changes greatly destroyed the excellent physical properties of original carbon nanotubes, especially as good conductive channels, which will increase the contact resistance between the components.

Generally, the nanocomposites comprised of carbon nanotubes and conducting polymers were fabricated by noncovalent combination methods via the interaction between the π-bonds of the aromatic rings of conducting polymers and the graphitic structures of carbon nanotubes. Recently, extensive efforts have been made to prepare carbon nanotubes−polyaniline nanocomposites. Yu et al. demonstrate the feasibility of the microemulsion route for the surface coverage of multiwall carbon nanotubes with conducting polymer.[14] Ginic-Markovic et al. introduced ultrasonically initiated, in situ emulsion polymerization to prepare polyaniline-wrapped carbon nanotubes.[15] Konyushenko et al. coated multiwall carbon nanotubes with protonated polyaniline in situ during the polymerization of aniline.[16] Wu et al. prepared the nanocomposites via the in situ polymerization, and carboxylic acid and acylchloride groups contained multiwalled carbon nanotubes were used as a core in the formation of tubular shells of doped polyaniline in its emeraldine salt form.[17,18] Yan et al. prepared the nanocomposites via electrostatic adsorption by rapid mixing of oxidized multiwall carbon nanotubes and polyaniline nanofibers in aqueous

* Corresponding author. E-mail: phqin@dhu.edu.cn (Z.-Y.Q.); zhumf@dhu.edu.cn (M.-F.Z.).
[†] State Key Laboratory for Modification of Chemical Fibers and Polymer Materials.
[‡] College of Material Science and Engineering.

10.1021/jp808582f CCC: $40.75
Published on Web 03/17/2009

colloids.[19] These works provide a successful strategy for fabricating nanocomposites of carbon nanotubes with conducting polymers.

It is well-known that the strong interaction between the aromatic rings of the polyaniline and the graphitic structures of carbon nanotubes would be a great benefit to the charge-transfer interaction between the two components. It implies that the nanotubes−polyaniline nanocomposites with good core−shell structures would be in an advantageous position. In this work, a facile method, ultrasonically assisted chemical oxidation polymerization, is presented to fabricate multiwall carbon nanotubes−polyaniline nanocomposites with good core−shell structures. A kind of the multiwall carbon nanotubes with minimal defects is applied as good templates for coating uniform polyaniline layers. Such carbon nanotubes can be obtained by treating commercial multiwall carbon nanotubes in the concentrated hydrochloric acid under ultrasonic irradiation, which has been demonstrated to have relatively smooth side-wall and closed ends, and very little carboxyl groups appear on carbon nanotubes. It is worth pointing out that more strong interaction between polyaniline and carbon nanotubes through the $\pi-\pi$ conjugation of the quinoid rings in polyaniline and the benzenoid rings of carbon nanotubes can be expected, which implies that the good core−shell structured nanocomposites can be obtained.[20] Also, the carbon nanotubes treated in mild hydrochloric acid would remain in the long tubes, which indicates that the remarkable mechanical properties of original carbon nanotubes would remain. We expect that this simple method could bring new opportunities for fabricating the uniformly and individually core−shell structured carbon nanotubes−polyaniline nanocomposites.

2. Experimental Details

Commercial multiwall carbon nanotubes (purity ≥95 wt %, 20−40 nm in diameter, 5−15 μm in length, CVD method, Shenzhen Nanoharbor Co.) were treated in concentrated hydrochloric acid under low power ultrasonic irradiation for 15 h at 70 °C, the resultant suspensions were subsequently filtrated and washed thoroughly with deionized water until the pH value was close to 7, and then the black solid powers were collected and dried in a vacuum at 80 °C.

The nanocomposites were synthesized by chemical oxidation polymerization of aniline in the presence of multiwall carbon nanotubes mentioned above. The solution of 1 M HCl 100 mL (containing treated MWNTs 0.5 g) was first stirred before the synthesis, and then the aniline monomers (0.025, 0.1, 0.5, and 2 g) in 1 M HCl were added into the MWNTs suspension (the content of MWNTs in the samples was 95, 80, 50, and 20 wt %, respectively). The mixtures were sequentially stirred in an ice bath under high power ultrasonic for one-half of an hour to make the mixture disperse homogeneously, and then the solution of 1 M HCl containing the oxidant $(NH_4)_2S_2O_8$ (ammonium peroxodisulphate, APS) was added one drop every 3 s (the mass ratio of APS to aniline was 1:1). The polymerization was carried out at 0 °C for 6 h, and then the acetone was added to terminate the reaction. The resulting products were filtered and washed with deionized water, and then dried under vacuum at 80 °C for 24 h. For comparison, pure polyaniline powers were prepared under conditions similar to those mentioned above.

The morphologies of the treated multiwall carbon nanotubes and the resulting nanocomposites were characterized by a JSM-5600LV (JEOL) scanning electron microscopy, H-800 (Hitachi) transmission electron microscopy, and JEM-2010 (JEOL) high-resolution scanning electron microscopy. The FTIR spectra were recorded on a Nicolet NEXUS 670 FTIR spectrometer, and the Raman spectra were recorded by a Renishaw spectrometer with a 50 mW Ar^+ laser at 514.5 nm. The crystal structures of the pure polyaniline and the resulting nanocomposites were studied by a RIGAKU D/Max-2550 PC X-ray diffraction instrument.

To measure the electrical conductivities of the nanocomposites, the pure polyaniline and resulting nanocomposites were first pressed into thin strips under 5 MPa at 60 °C, and then the electrical conductivities were measured by two-point probe method at room temperature. To study their electrochemical properties, the nanocomposites were also pressed onto the nickel mash current collector. The cyclic voltammogram was recorded on a CHI 1000A electrochemical working station (CH Instrument, Inc.) in 0.1 M H_2SO_4 aqueous solution by using a Pt wire as the counter electrode and Ag/AgCl as the reference electrode.

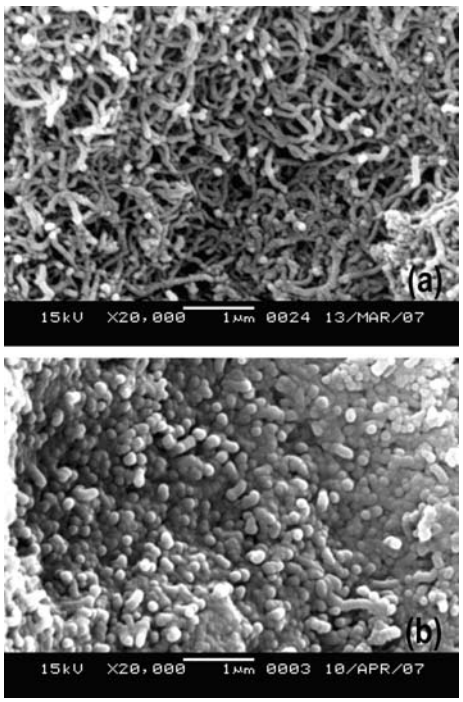

Figure 1. SEM images of (a) treated MWNTs and (b) 50 wt % MWNTs containing a composite with core−shell structure.

3. Results and Discussion

The SEM images for the treated multiwall carbon nanotubes and multiwall carbon nanotubes polyaniline nanocomposites (50 wt % MWNTs contained) were shown in Figure 1. The carbon nanotubes treated in concentrated hydrochloric acid were shown in Figure 1a, and the tangled rope-like tubes with smooth surface and closed ends as expected can be observed. The nanocomposites corresponding to 50 wt % MWNTs content were shown in Figure 1b; the increasing thickness of nanotubes can be observed obviously, and the nanotubes exhibited similar diameters, which indicated the uniform formation of polyaniline layers on carbon nanotubes. These results showed clearly the nanocomposites with good core−shell structures had been fabricated successfully.

The morphology of the resulting nanocomposites was observed using electron microscopy. Figure 2 showed the typical TEM images of the MWNTs and various carbon nanotubes−polyaniline composites. As shown in Figure 2a, carbon nanotubes treated in concentrated hydrochloric acid remained in the long tubes with the diameter of about 20−30 nm. Also, the HR-TEM image in Figure 2b showed a smooth wall of the carbon nanotubes with the regular configuration of the graphite layers; it can hardly

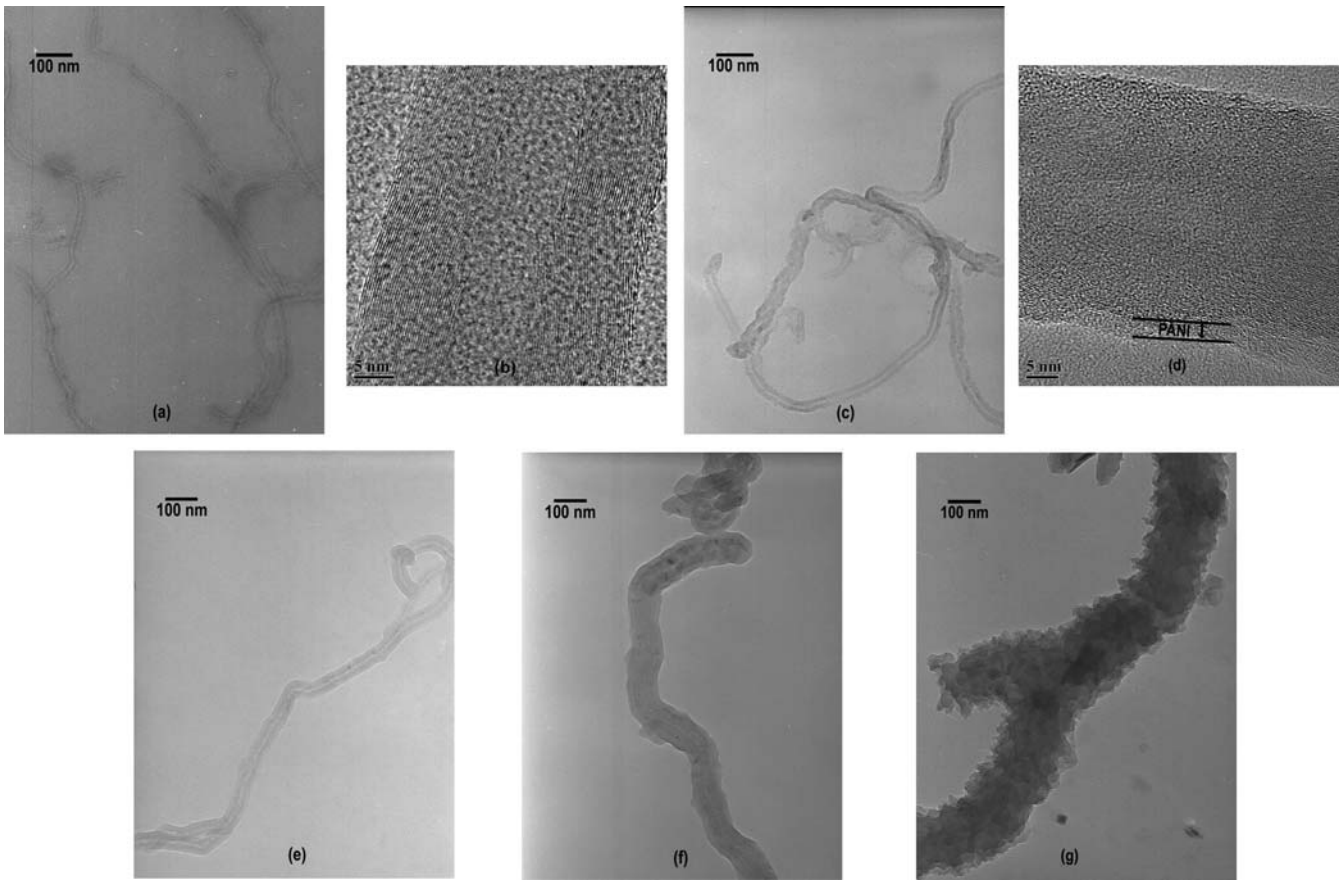

Figure 2. TEM images of (a) treated MWNTs, (c) 95 wt % MWNTs composite, (e) 80 wt % MWNTs composite, (f) 50 wt % MWNTs composite, (g) 20 wt % MWNTs composite; and HR-TEM images of (b) treated MWNTs, (d) 95 wt % MWNTs composite.

find the defects such as amorphous carbon. For the nanocomposites with 95 wt % MWNTs content, little change in the dimension of nanotubes and no obvious particles appeared on the nanotubes surfaces, which indicated that polyaniline layers were very thin, uniform, and tightly stacked on the tubes as shown in Figure 2c; in its HR-TEM image shown in Figure 2d, the outer layer of the PANI, which was 2−5 nm in thickness, can be seen clearly. In Figure 2e,f, with the decreasing of carbon nanotubes content from 80 to 20 wt %, it can be clearly observed that the whole carbon nanotubes were covered by uniform polyaniline layers, which indicated the formation of apparent core−shell structures. This result showed that a more planar conformation of polyaniline formed on the surfaces of carbon nanotubes with minimized defects. The thickness of polyaniline layers changed from about 5 nm for 80 wt % MWNTs content to about 20−25 nm for 50 wt % MWNTs content. By varying the ratio of aniline monomer and carbon nanotubes, the thickness of polyaniline layer can be effectively controlled. However, when the ratio of aniline monomers and carbon nanotubes further increased, that is to say, the MWNTs content in the nanocomposites decreased, the smooth surfaces of nanotubes became rough. For the nanocomposites with 20 wt % MWNTs content, the thickness of the polyaniline layers increased to 40−50 nm. Although scarcely large polyaniline particles can be found in Figure 2g, the outer layers were no longer smooth, and the nanotubes looked like a caterpillar, similar to Wu's reported result.[18] It was worth pointing out that in their works, carboxylic groups containing multiwalled carbon nanotubes were applied as templates, and polyaniline layers on carbon nanotubes would form slowly on nanotubes with large diameters, which was opposite of our observation. The behavior could be attributed to the difference in the interaction between the polyaniline and the carbon nanotubes; more planar and compact polyaniline layers would be formed on carbon nanotubes with minimal defects.

The typical FT-IR spectra of pure polyaniline, treated MWNTs, and the resulting nanocomposites were shown in Figure 3. These spectra were in good agreement with previously reported results.[15−18,21−23] The main transmission bands of MWNTs in Figure 3a situated at 1580 and 3460 cm^{-1} were attributed to the stretching of the C═C in quinoid ring and the stretching vibration of the O−H.[19] As compared to the peaks of polyaniline, the specific peak of carbon nanotubes was relatively weak, and almost no groups such as carboxyl or carbonyl groups appeared clearly in the treated carbon nanotubes, which implied that carbon nanotubes used in our work had minimized defects.

In Figure 3b, the main bands situated at 820, 1120, 1235, 1280, 1470, and 1555 cm^{-1} in the resulting nanocomposites were attributed to the following vibrations: bending of C−H (out of plane) in benzene ring π-disubstituted, stretching of *C*═N (−*N*═quinoid═N−), stretching vibration of the $CN^{\cdot+}$ in the polaron structure of polyaniline, stretching of C−N secondary aromatic amine, stretching vibration of C═C in benzenoid ring, and stretching vibration of C═C in quinoid ring, respectively.[15−18,21−23] As is observed commonly for multiwall carbon nanotubes−polyaniline composites, all spectra exhibited the clear presence of quinoid and benzenoid ring vibrations at 1470 and 1555 cm^{-1}, respectively, indicating the presence of oxidation state of polyaniline (ES).[16,17] As compared to the pure polyaniline, an inversed intensity ratio of 1555/1470 cm^{-1} shown in the spectrum of the nanocomposites revealed more quinoid rings in the nano-

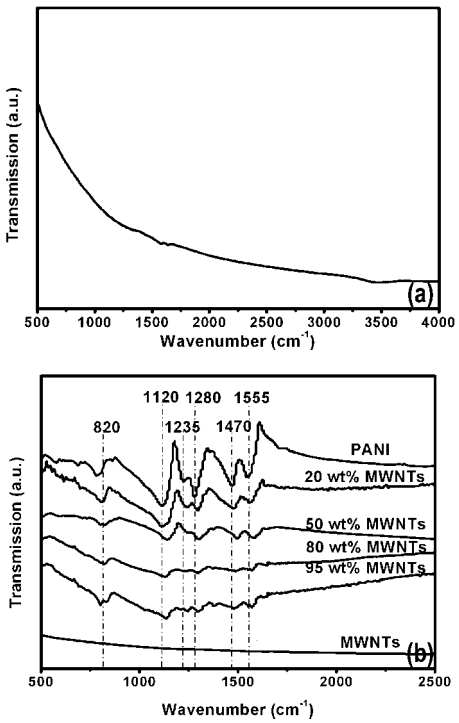

Figure 3. FTIR spectra of (a) treated MWNTs and (b) treated MWNTs, PANI, and the resulting nanocomposites.

composites. It can be obviously found that the ratio of 1555/1470 cm^{-1} decreased rapidly with the decreasing of the MWNTs contents from 95 to 50 wt %. The observed increase in quinoid rings in structure for the resulting nanocomposites indicated that the carbon nanotubes interact more strongly with the quinoid than with the benzene ring.[21,24]

We noted that some typical bands of polyaniline moved to relatively high frequency with the increasing of the contents of carbon nanotubes in the nanocomposites as shown in Figure 3. As compared to the peak position of pure polyaniline, the position of the *C*═N(−*N*═quinoid═N−) band of polyaniline moved from 1120 to 1140 cm^{-1} in composites, stretching vibration of the C−$N^{\cdot+}$ in the polaron structure of polyaniline at 1235 cm^{-1} moved to 1250 cm^{-1}, stretching vibration of C═C in benzenoid ring of polyaniline at 1470 cm^{-1} moved to 1476 cm^{-1} in the nanocomposites with 20 wt % MWNTs content, then to 1496 cm^{-1} in the following two composites, and the stretching vibration of C═C in the quinoid ring of polyaniline at 1565 cm^{-1} moved to 1575 cm^{-1} in composites, respectively. It is supposed that the polyaniline chains were constrained to grow around the tubes, and the constrained motion of the chains restricted modes of vibrations in polyaniline, which led the frequencies of vibrations to move to a relatively high wavenumber. As compared to other band shifts, the more obvious change in the benzenoid ring vibration can be observed. When the benzenoid rings of polyaniline transformed into quinoid rings, making the interaction more intense between polyaniline and carbon nanotubes, the vibration of polyaniline molecules would be restricted strongly, which led to relatively high wavenumber band shifts.[19,25−27]

The strong characteristic band appearing around 1140 cm^{-1} was described as the "electron-like band" and considered to be a measurement of delocalization of electrons.[28] This increase was expected to be relative to the interaction between the MWNTs and polyaniline, which could increase the effective degree of electron delocalization. It is well-known that the strong interaction between the carbon nanotubes and polyaniline would

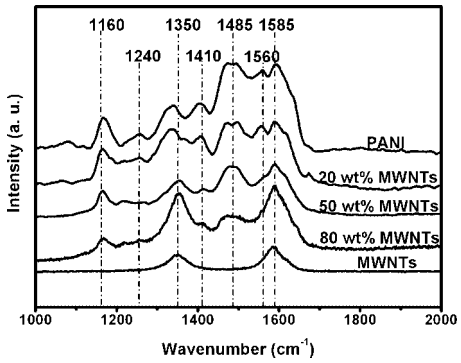

Figure 4. Raman spectra of MWNTs, PANI, and the resulting nanocomposites.

facilitate a charge-transfer process between the components of the system, which contributed to the increasing of the conductivity of the nanocomposites.

On the basis of our TEM and FTIR results, we would like to propose the process of the polymerization as follows: at the beginning of the polymerization, the strong $\pi-\pi^*$ conjugation between the MWNTs and aniline facilitates the adsorbing of aniline on the tube, and then the MWNTs with minimized defects acted as the template for the formation of polyaniline layers. Because of the presence of carbon nanotubes with minimized defects, compact polyaniline layers with more planar conformation would form on the nanotube surface, even when 80 wt % aniline was loaded. With the increasing of the polyaniline layers, the interaction between the carbon nanotubes and the aniline decreased gradually, and so the interaction between the polymer and the monomer became the leading interaction. The reaction would take place preferentially at some active spots on the PANI layer during the later stage of polymerization, and then the caterpillar-like structure appeared on the outer layers of nanotubes.

To further confirm the above interaction had taken place between the MWNTs and polyaniline, we investigated Raman spectra of MWNTs, pure polyaniline, and the resulting nanocomposites as shown in Figure 4. The strong peak of the MWNTs at 1585 cm^{-1} (G lines) was the Raman-allowed phonon high frequency E_{2g} first-order mode, and the disorder-induced peak at 1350 cm^{-1} (D lines).[15] For polyaniline and the resulting composites, C−H bending of the quinoid ring at 1160 cm^{-1}, C−H bending of the benzenoid ring at 1240 cm^{-1}, C═C stretching of the quinoid ring at 1485 cm^{-1}, and stretching of the benzenoid ring at 1590 cm^{-1} were observed, respectively, revealing the presence of doped polyaniline structures.[14] As compared to the spectra of pure polyaniline, the C−$N^{\cdot+}$ stretching peak gradually shifts to the high wavenumber from 1339 to 1343 cm^{-1} in the nanocomposites with 20 wt % MWNTs content, then to 1350 cm^{-1} in the nanocomposites with relatively high MWNT content, while the intensity increased gradually. This also implied that with the increasing MWNTs, the interaction between the MWNTs and the polyaniline increased gradually, which was illustrated by our FTIR results. In addition, the increase of the C═C stretching of quinoid ring at 1485 cm^{-1} in composites as compared to pure polyaniline indicates the increasing of protonic acid doping in the presence of MWNTs.

Figure 5 presented the X-ray diffraction data of MWNTs, polyaniline, and the resulting nanocomposites. For MWNTs, the diffraction peaks were observed at 25.88° and 42.72°, corresponding to graphite-like structure.[29] Meanwhile, for polyaniline, the characteristic peaks appeared at 15.04°, 20.48°,

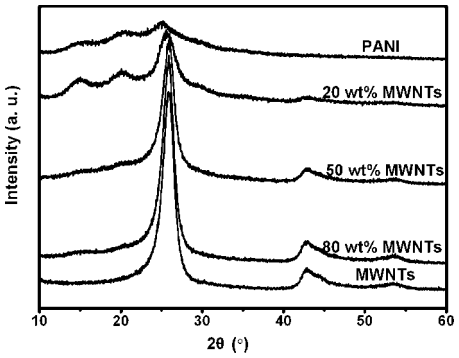

Figure 5. XRD patterns of MWNTs, PANI, and the resulting nanocomposites.

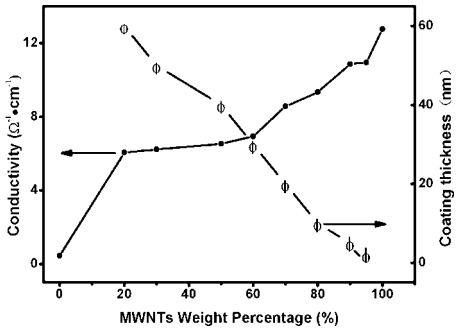

Figure 6. Conductivity of the resulting nanocomposites and thickness of polyaniline layers on carbon nanotubes for various MWNTs contents.

24.80°, and 29.70°, corresponding to (011), (020), (200), and (022) reflections of polyaniline in its emeraldine salt form.[15] The XRD pattern of the nanocomposites showed crystal peaks similar to those obtained from pure polyaniline, indicating that no additional crystalline order was introduced into the nanocomposites. The interaction between the MWNTs and aniline would decrease with the increasing thickness of polyaniline layers. When comparing the nanocomposites with other MWNTs content, the obvious characteristic peaks of polyaniline in the nanocomposites for 20 wt % MWNTs content that appeared at 15.04° and 20.48° can be ascribed to the formation of more integrated crystal appearing on the outer layers of nanotubes because of less interaction between the two components.

The conductivity of the polyaniline, MWNTs, and the resulting nanocomposites was measured by the two-point probe method, and the results were shown in Figure 6. With increasing MWNTs content, the conductivities for the resulting nanocomposites increased by more than 1 order of magnitude as compared to the pure polyaniline (0.45 Ω^{-1} cm^{-1}). Besides carbon nanotubes serving as an effective "conducting bridge", the enhancing of conductivities of the nanocomposites also benefited from the dopant effect and charge transfer from the quinoid units of polyaniline to the carbon nanotubes, in which the carbon nanotubes act as good electron acceptor and polyaniline as a good electron donor.[28] However, the conductivities of the nanocomposites were still lower than that of pure carbon nanotubes, even as high to 95 wt % MWNTs were loaded.

The electrochemical properties of the resulting nanocomposites were evaluated by cyclic voltammetry (CV) as shown in Figure 7. It showed a typical double-layer capacity behavior of carbon nanotubes, which benefited from their large surface area. The CV curve of carbon nanotubes was nearly a rectangle,

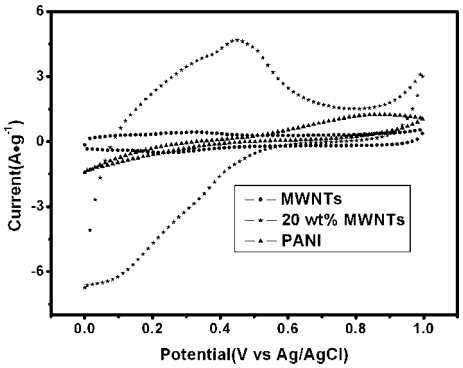

Figure 7. Cyclic voltammogram of MWNTs, polyaniline, and the resulting nanocomposites with 20 wt % MWNTs content as working electrodes at a scan rate of 5 mV/s in 0.1 M H_2SO_4 aqueous electrolyte.

which indicated an ideal supercapacitor behavior. Unfortunately, the specific capacitance of pure carbon nanotubes was only 65 F/g at the scan rate of 5 mV/s. For the pure polyaniline, its specific capacitance was not more than 80 F/g. However, for the nanocomposite with 20 wt % MWNTs content, its specific capacitance as high as 262 F/g can be obtained under nonoptimized condition. This improvement can be attributed to the core−shell structure increased effectively the surface area of the electrode, which increased greatly the contact of the electrode and the electrolyte; by the way, the integrated core−shell structure facilitated the flowing of electrons. In addition, the newly fabricated carbon nanotubes−polyaniline nanocomposites with uniform core−shell structures might be of significant interest in the applications of an energy-conversion system such as supercapacitors, solar cells, hydrogen production by electrolysis, microelectromechanical systems, multifunctional sensor, and electromagnetic shielding devices.

4. Conclusion

In summary, we used multiwall carbon nanotubes with minimal defects as templates, and we successfully fabricated carbon nanotubes−polyaniline nanocomposites with core−shell structures by ultrasonic assisting in situ polymerization. The templates can be obtained easily by ultrasonically assisted concentrated HCl treatment of commercial MWNTs under reflux condition. It was demonstrated that such MWNTs could act as a good template for the formation of uniform core−shell structured carbon nanotubes−polyaniline nanocomposites; the layer thickness of coating can be controlled effectively by means of simply varying the ratio of aniline monomer and carbon nanotubes. The characteristic results indicated that the presence of carbon nanotubes with minimized defects induced the formation of compact polyaniline layers with more planar conformation, even when 80 wt % aniline was loaded. The effective site-selective interaction between the π-bonds in the aromatic ring of the polyaniline and the graphitic structure of carbon nanotubes should strongly facilitate the charge-transfer reaction between the two components. The improvements on electrical and electrochemical properties were observed for such nanocomposites with core−shell structures. The preliminary results showed that the above nanocomposites exhibited extensive potential applications as high-efficiency electrode materials.

Acknowledgment. We greatly acknowledge financial support from the Shanghai Pujiang Program (07pj14005) and Shanghai Nano Special Projects (0652nm041).

References and Notes

(1) Terrones, M. *Annu. Rev. Mater. Res.* **2003**, *33*, 419–501.
(2) Panhuis, M.; Sainz, R.; Innis, P. C.; Kane-Maguire, L. A. P.; Benito, A. M.; Martinez, M. T.; Moulton, S. E.; Wallace, G. G.; Maser, W. K. *J. Phys. Chem. B* **2005**, *109*, 22725–22729.
(3) Long, Y. Z.; Yin, Z. H.; Chen, Z. J. *J. Phys. Chem. C* **2008**, *112*, 11507–11512.
(4) Panhuis, M. *J. Mater. Chem.* **2006**, *16*, 3598–3605.
(5) Yamamoto, T. *Macromol. Rapid Commun.* **2002**, *23*, 583–606.
(6) Liu, X. L.; Ly, J.; Han, S.; Zhang, D. H.; Requicha, A.; Thompson, M. E.; Zhou, C. W. *Adv. Mater.* **2005**, *17*, 2727.
(7) Li, W. K.; Chen, J.; Zhao, J. J.; Zhang, J. R.; Zhu, J. J. *Mater. Lett.* **2005**, *59*, 800–803.
(8) Downs, C.; Nugent, J.; Ajayan, P. M.; Duquette, D. J.; Santhanam, S. V. *Adv. Mater.* **1999**, *11*, 1028–1031.
(9) Wu, M. Q.; Snook, G. A.; Gupta, V.; Shaffer, M.; Fray, D. J.; Chen, G. Z. *J. Mater. Chem.* **2005**, *15*, 2297–2303.
(10) Ali, S. R.; Ma, Y. F.; Parajuli, R. R.; Balogun, Y.; Lai, W. Y. C.; He, H. X. *Anal. Chem.* **2007**, *79*, 2583–2587.
(11) Germain, J.; Fréchet, J. M. J.; Svec, F. *J. Mater. Chem.* **2007**, *17*, 4989–4997.
(12) Cochet, M.; Maser, W. K.; Benito, A. M.; Callejas, M. A.; Martinez, M. T.; Benoit, J. M.; Schreiber, J.; Chauvet, O. *Chem. Commun.* **2001**, *40*, 1450–1451.
(13) Tasis, D.; Tagmatarchis, N.; Bianco, A.; Prato, M. *Chem. Rev.* **2006**, *106*, 1105–1136.
(14) Yu, Y. J.; Che, B.; Si, Z. H.; Li, L.; Chen, W.; Xue, G. *Synth. Met.* **2005**, *150*, 271–277.
(15) Ginic-Markovic, M. G.; Matisons, J.; Cervini, R.; Simon, G. P.; Fredericks, P. M. *Chem. Mater.* **2006**, *18*, 6258–6265.
(16) Konyushenko, E. N.; Stejskal, J.; Trchova, M.; Hradil, J.; Kovarova, J.; Prokes, J.; Cieslar, M.; Hwang, J. Y.; Chen, K. H.; Sapurina, I. *Polymer* **2006**, *47*, 5715–5723.
(17) Wu, T. M.; Lin, Y. W.; Liao, C. S. *Carbon* **2005**, *43*, 734–738.
(18) Wu, T. M.; Lin, Y. W. *Polymer* **2006**, *47*, 3576–3582.
(19) Yan, X. B.; Han, Z. J.; Yang, Y.; Tay, B. K. *J. Phys. Chem. C* **2007**, *111*, 4125–4127.
(20) Fan, Q. Q.; Qin, Z. Y.; Liang, X.; Li, L.; Wu, W. H.; Zhu, M. F., submitted.
(21) Baibarac, M.; Baltog, I.; Lefrant, S.; Mevellec, J. Y.; Chauvet, O. *Chem. Mater.* **2003**, *15*, 4149–4155.
(22) Feng, W.; Bai, X. D.; Lian, Y. Q.; Liang, J.; Wang, X. G.; Yoshino, K. *Carbon* **2003**, *41*, 1551–1557.
(23) Zengin, H.; Zhou, W. S.; Jin, J. Y.; Czerw, R.; Smith, D. W.; Echegoyen, L.; Carroll, D. L.; Foulger, S. H.; Ballato, J. *Adv. Mater.* **2002**, *14*, 1480–1483.
(24) Do Nascimento, G. M.; Corio, P.; Novickis, R. W.; Temperini, M. L. A.; Dresselhaus, M. S. *J. Polym. Sci., Part A: Polym. Chem.* **2005**, *43*, 815–822.
(25) Yang, M. J.; Koutsos, V.; Zaiser, M. *J. Phys. Chem. B* **2005**, *109*, 10009–10014.
(26) Chen, J.; Liu, H.; Weimer, W. A.; Halls, M. D.; Waldeck, D. H.; Walker, G. C. *J. Am. Chem. Soc.* **2002**, *124*, 9034–9035.
(27) Chen, R. J.; Zhang, Y. G.; Wang, D. W.; Dai, H. J. *J. Am. Chem. Soc.* **2001**, *123*, 3838–3839.
(28) Boyer, M.-I.; Quillard, S.; Rebourt, E.; Louarn, G.; Buisson, J. P.; Monkman, A.; Lefrant, S. *J. Phys. Chem. B* **1998**, *102*, 7382–7392.
(29) Liu, S. W.; Yue, J.; Wehmschulte, R. J. *Nano Lett.* **2002**, *2*, 1439–1442.

JP808582F